INTERNATIONAL SOCIETY FOR
SOIL MECHANICS AND
GEOTECHNICAL ENGINEERING

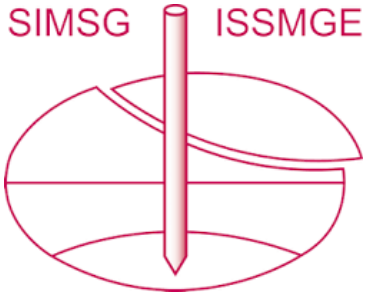

This paper was downloaded from the Online Library of the International Society for Soil Mechanics and Geotechnical Engineering (ISSMGE). The library is available here:

https://www.issmge.org/publications/online-library

This is an open-access database that archives thousands of papers published under the Auspices of the ISSMGE and maintained by the Innovation and Development Committee of ISSMGE.

Study on long-term subsidence of soft clay due to 2007 Niigata Prefecture Chuetsu-Oki Earthquake

Étude sur l'affaissement à long terme d'argile molle dû au tremblement de terre de la préfecture de Niigata Chuetsu-Oki en 2007

Isobe K., Ohtsuka S.
Nagaoka University of Technology

ABSTRACT: In the 2007 Niigata Prefecture Chuetsu-Oki Earthquake, ground liquefaction was particularly prominent at the foot of sand dunes and at old river channels in the area affected. Although extensive damage to clayey ground was not seen immediately after the tremor, long-term subsidence has been observed in such ground in the Shinbashi district of Kashiwazaki City. Against such a background, the present study was conducted to investigate the mechanism of this long-term subsidence through ground investigations in the form of a boring survey and indoor element tests on soil samples. The results showed that the samples were very soft and relatively highly structured. In the study's second part, ground subsidence was simulated via elasto-plastic analysis of soil coupled with classical consolidation theory by using FEM. In the simulation, the Cyclic Mobility model developed by Zhang et al. (2007), which incorporates the concepts of subloading and superloading (as described by Hashiguchi and Ueno (1977) and Asaoka et al. (2002)) was used as the constitutive model with parameters determined in line with the element test results. Based on the outcomes of the simulation, the post-quake behavior of soft clay and the related mechanism were elucidated, and the progress of subsidence was predicted.

RÉSUMÉ : Lors du Tremblement de terre au Chuetsu-Oki (Préfecture de Niigata) à 2007, la liquéfaction des sols a été particulièrement importante au pied des dunes de sable et aux canaux des rivières anciennes dans la zone affectée. Bien que des dégâts significatifs du terrain argileuse n'aient pas été vus tout de suite après le tremblement de terre, le tassement à long terme a été observé dans le quartier de Shinbashi, à Kashiwazaki. Dans un tel contexte, l'étude actuelle a été effectuée pour étudier les mécanismes de ce tassement à long terme à traverse d'une étude par carottage et des tests au laboratoire sur des échantillons de sol. Les résultats ont montré que les échantillons étaient très doux et relativement très structuré. Dans la deuxième partie de cette étude, l'affaissement du sol a été modélisé par le couplage de sol-eau et des analyses élasto-plastique à l'aide de l'élément finis. Dans la simulation, le modèle de mobilité cyclique développé par Zhang et al. (2007), qui intègre les concepts de sub-charge et super-charge (comme étant décrit par Hashiguchi et Ueno (1977) et Asaoka et al. (2002)) a été utilisé comme loi de comportement en utilisant des paramètres déterminés par des essais expérimentaux. En se basant sur des résultats de la modélisation, le comportement post-sismique de l'argile molle et les mécanismes associés ont été élucidés, et l'évolution du tassement dans le temps a été aussi prédit.

KEYWORDS: earthquake, soft clay, long-term ground subsidence, over consolidation, soil structure, soil-water coupling, FE analysis

1 INTRODUCTION

The Niigata Prefecture Chuetsu-Oki Earthquake that hit Japan on July 16th, 2007, killed 11 people and damaged more than 6,000 residences. The quake registered 6.8 on the magnitude scale of the Japan Meteorological Agency (JMA), and a Kyoshin Net (K-net) accelerograph measured a maximum ground acceleration of 813 Gal. The results of a ground subsidence survey conducted by Niigata Prefecture officials in the Shimbashi district of Kashiwazaki City indicated that long-term ground subsidence has continued there since the quake occurred.

To investigate the cause of earthquake-related long-term subsidence in soft clay ground, boring investigation involving standard penetration tests (SPTs) was conducted in this study in the vicinity of a site where ground subsidence was observed. Static and cyclic CU tri-axial tests were also carried out to clarify the mechanical characteristics and liquefaction strength of Kashiwazaki clay. Subsequently, soil-water coupling elasto-plastic finite element analysis was performed with soil parameters determined from the above element test results to simulate the observed subsidence. In this study, the cause of long-term subsidence in soft clay was discussed and future subsidence was mathematically predicted based on the results of simulation.

2 OVERVIEW OF GEOGRAPHICAL CONDITIONS IN KASHIWAZAKI CITY

Figure 1 (a) shows a map of the city highlighting cumulative ground subsidence both before 2009 and after the earthquake, and Figure 1 (b) shows a terrain classification map of the area. The zone in which ground subsidence was observed before the quake is mainly located on land consisting of soft alluvial clay, while that in which it developed after the quake is located near the sea and is mostly covered by the above-mentioned area. Stratified subsidence and ground water levels were measured by Niigata Prefecture officials in the Shinbashi district (marked as B in Figure 1 (b)) from 1989 to 2011, and Figure 2 shows temporal changes in ground water level and cumulative subsidence to a depth of 23 m. It can be seen from the figure that subsidence progressed rapidly after the quake of 2007 and continued for over three years. However, this was not caused by consolidation of soft clay due to changes in the ground water level because no drastic changes in water level were observed in the area. To pinpoint the cause, boring investigation involving standard penetration tests (SPTs) was carried out in the vicinity of a site where ground subsidence was observed, and the area's soft clay was sampled. Figure 3 shows geological columns of the area based on the results of the authors' boring investigation and information from the Hokuriku Geological System database. Land in the Shinbashi district consists mainly of very

soft clay with N values ranging from 0 to 2. Small pieces of weathered shells are seen from a depth of around 11.0 m, and more significant shell presence is observed from around 14.0 m. The soft clay layer extends to a depth of 21 m and sits on a silt layer with an N value of approximately 10. The silt layer extends to a depth of 50 m with N values of more than 50, making it suitable as engineering foundation ground. In contrast, the soft clay layer in the area around point D is thinner than that around point C. Sand dunes with N values of more than 10 cover the clay and slit layers at point A near the sea. It is clear that the zone in which extensive post-quake subsidence was observed corresponds to the area of the thick alluvial cl ay layer.

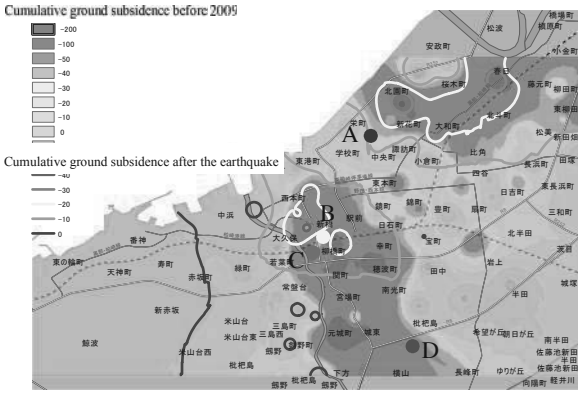

Figure 1. (a) Cumulative ground subsidence before 2009 and in Kashiwazaki City.

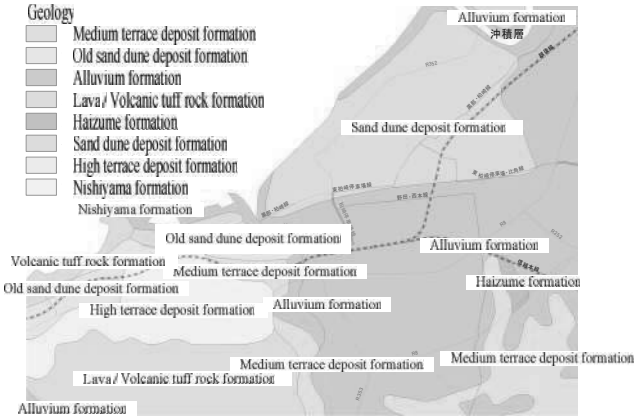

Figure 1. (b) Kashiwazaki City terrain classification.

3 SOFT CLAY SAMPLE PHYSICAL PROPERTIES AND MECHANICAL CHARACTERISTICS

As there is a difference in the amount of contamination by weathered shells between the shallow and deep clay layers, intact samples were obtained from depths of G.L. -16.7 - 19.0 m and G.L. -9.0 m - 11.7 m in the Shinbashi district of Kashiwazaki City. The physical properties are shown in Tables 1. It can be seen that samples from both depths have a high natural water content and plasticity index, and consist of more than 50% clay.

Subsequently, oedometer tests and static and repeated CU tri-axial tests were carried out to clarify the consolidation characteristics of the samples from both depths. Two specimens types were created: (1) intact specimens, and (2) reconstituted specimens made from a slurry sample with water added after the above tests. To achieve a high degree of saturation, vacuum conditions were applied to both the cell and the sample interior. The specimen was isotropically consolidated for 18 hours under confining pressures of 50 - 200 kPa. In order to examine static shear strength and liquefaction strength, static and cyclic tests were performed by applying deviator stress at a loading rate of 0.021 mm/min and uniform sinusoidal cycles of deviator stress at a frequency of 0.01 Hz with a varying cyclic stress ratio under constant cell pressure.

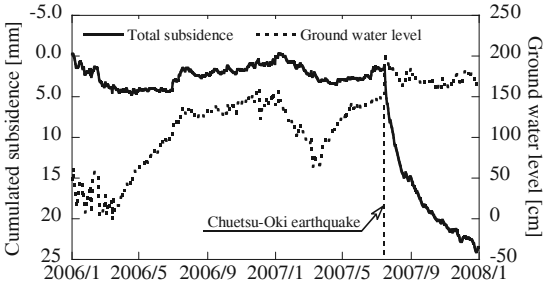

Figure 2. Temporal changes in ground water level and cumulative subsidence to a d epth of 23 m (from 2006 to 2008).

Table 1. Kashiwazaki clay physical properties.

		Clay
Specific gravity [g/cm^3]	G_s	2.68
Plasticity index [%]	I_p	48.6
Liquid limit [%]	w_l	87.0
Plastic limit [%]	w_p	38.4
Natral water content [%]	w_n	73.5

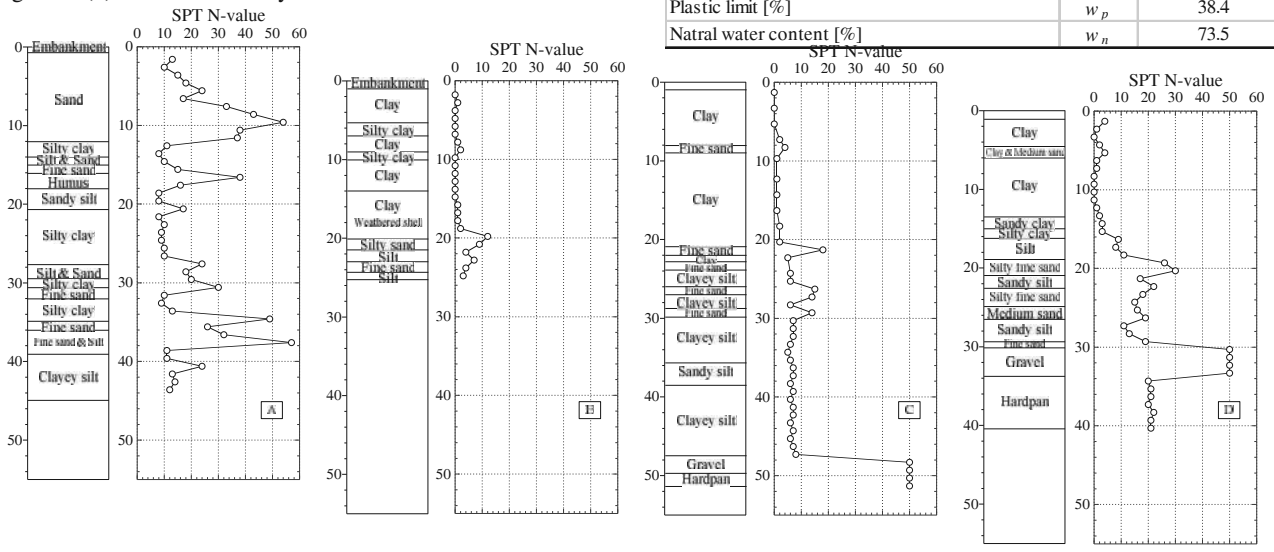

Figure 3. Geological columns for Kashiwazaki City based on boring investigation carried out by the authors and information from the Hokuriku Geological System database (A – D correspond to the areas on the map shown in Figure 1 (a)).

Figure 4 shows the *e*-log*p'* relationship observed in the oedometer tests for these specimens from the shallow and deep layers. It can be seen that the intact specimens from each layer exhibited characteristics of high compression after application of consolidation yield pressure (about 140 kPa) compared to those of the reconstituted specimens. The compression index ratio (defined as the ratio of the compression index of the intact samples to that of the reconstituted samples) values for the shallow and deep layers were 1.40 and 2.25, respectively. According to Asaoka et al. (2000), clay obtained from deep layers is characterized by a light structure. The layers in the vicinity of the ground surface at the site appear to have been over-consolidated, as the consolidation yield stress of samples from both depths was about 140 kPa.

Figure 5 shows the relationship between deviator stress and axial strain, and the effective stress paths of the static CU tri-axial tests for the intact specimens sampled from both layers. For the deep-layer samples with confining pressure values of 50 kPa and 100 kPa, the mean effective stress decreased with greater excess pore water pressure (EPWP) and the mean effective stress increased after the stress path reached the critical state line (CSL), meaning that the volume of the soil skeleton decreases after the deviator stress turned down. This indicates that the samples exhibited compression-softening behavior and were lightly structured. However, such behavior was not observed in the samples with confining pressure values of 150 kPa due to structural collapse during the isotropic consolidation process up to more than consolidation yield stress before shearing. Conversely, the samples from the shallow layer showed typical behavior of over-consolidated soils, and the deviator stress when the stress path reached the CSL was slightly greater than that for the sample from the deep layer subjected to the same conditions of confining pressure loading.

4 NUMERICAL SIMULATION

The Cyclic Mobility model developed by Zhang et al. (2007), which incorporates the concepts of subloading and superloading as described by Hashiguchi and Ueno (1977) and Asaoka et al. (2002), was used as the constitutive model. A brief description of its yielding surfaces and the evolution rule for the anisotropic stress tensor, the degree of structure and overconsolidation is given as:

$$f(p',\eta^*,\zeta)+\ln R' - \ln R - \frac{\varepsilon_v^p}{MD} = \ln\frac{p'}{p_0'} + \ln\frac{M^2-\zeta^2+\eta^{*2}}{M^2-\zeta^2} + \ln R^* - \ln R - \frac{\varepsilon_v^p}{MD} = 0 \quad (1)$$

$$\dot{\boldsymbol{\beta}} = \frac{b_r(b_l M-\zeta)}{D}\sqrt{\frac{2}{3}}\left\|\boldsymbol{D}_s^p\right\|\frac{\hat{\boldsymbol{\eta}}}{\|\hat{\boldsymbol{\eta}}\|} = \lambda\frac{\sqrt{6}b_r(b_l M-\zeta)}{D(M^2-\zeta^2+\eta^{*2})p'}\hat{\boldsymbol{\eta}} \quad (2)$$

$$\dot{R}^* = \frac{a}{D}R^*(1-R^*)\sqrt{\frac{2}{3}}\left\|\boldsymbol{D}_s^p\right\| = \lambda\frac{2aR^*(1-R^*)\eta^*}{D(M^2-\zeta^2+\eta^{*2})p'} \quad (3)$$

$$\dot{R} = -\frac{m}{D}\left\{\frac{(p'/p_0')^2}{(p'/p_0')^2+1}\right\}\ln R\,\|\boldsymbol{D}^p\| + R\frac{\eta}{M}\frac{\partial f}{\partial\boldsymbol{\beta}}\cdot\dot{\boldsymbol{\beta}} = \lambda\frac{-m\ln R\sqrt{6\eta^{*2}+\frac{1}{3}(M^2-\zeta^2)^2}}{D(M^2-\zeta^2+\eta^{*2})p'}\left\{\frac{(p'/p_0')^2}{(p'/p_0')^2+1}\right\} + R\frac{\eta}{M}\frac{\partial f}{\partial\boldsymbol{\beta}}\cdot\dot{\boldsymbol{\beta}} \quad (4)$$

Figure 5 shows the performance of the element simulation for the behavior of clay in undrained static compression tests. The values of the material parameters and the initial conditions used in the simulations are listed in Table 2. It can be seen from this information that the simulation results exhibit close correspondence to the experimental results except in the case of high confining pressure. Soil was not sampled from this layer in previous field investigations because no subsidence was observed there. In this simulation, the values for typical silt such as Fujinomori clay were used as parameters for the silt layer.

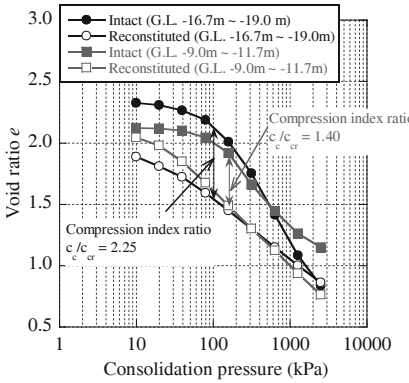

Figure 4. *e*-log*p'* relationship for intact and reconstituted samples from the shallow and deep layers.

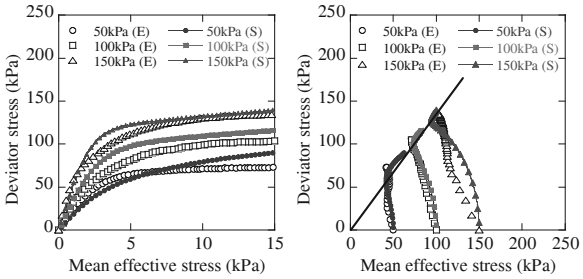

Figure 5(a). Static triaxial test simulation for intact samples from the shallow layer

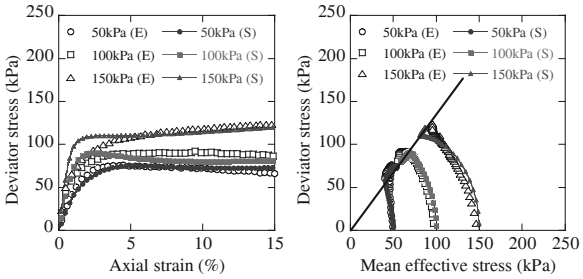

Figure 5(b). Static triaxial test simulation for intact samples from the deep layer

Table 2. Soil parameters used in the simulation

		Shallow layer	Deep layer	Silt
Compression index	□	0.264	0.214	0.104
Swelling index	□	0.080	0.031	0.010
Stress ratio at critical state	R_f	3.500	3.500	3.000
Void ratio (p' = 98 kPa on N.C.L)	N	1.610	1.540	0.920
Poisson's ratio	□	0.330	0.330	0.200
Degradation parameter of overconsolidation state	m	5.000	15.000	2.200
Degradation parameter of structure	a	2.200	1.200	0.100
Evolution parameter of anisotropy	br	0.100	0.100	0.100
Initial mean effective stress [kPa]	p'	8 ~ 73	78~111	117~295
Initial degree of structure	R_0^*	0.950	0.600	0.100
Initial degree of overconsolidation	$1/R_0$	1.9~19	1.3~1.8	2.500
Initial anisotropy	□	0.000	0.000	0.000
Permiablity [m/sec]	k	1.00E-09	1.00E-09	1.00E-07
Saturated unit weight [kN/m^3]	□$_{sat}$	15.36	15.66	17.00
Unit weight under water [kN/m^3]	□'	5.36	5.66	7.00

The DBLEAVES soil-water coupling FE analysis code (Ye et al., 2007) was used in the study's simulation. The FE model is simplified to a one-dimensional column of soil elements measuring 1 m in width, length and height as shown in Figure 6. Here it is assumed that the ground is level, and the effects of terrain geometry are not taken into account in the simulation. The boundary conditions are as follows: (a) The bottom of the ground is fixed. (b) In dynamic analysis, an equal-displacement-boundary condition is applied between nodes in two sides of the ground; when the analysis is shifted to consolidation, the boundary condition is changed to a fixed one. (c) The ground surface is set with a drainage condition, while the other surfaces are impermeable.

In the numerical simulation, the process of shaking is represented via dynamic soil-water coupled analysis, while the process of EPWP dissipation is simulated via static consolidation analysis. As the whole process is continuous, it should be simulated as an ongoing sequence. The simulation is divided into two stages as follows: (a) dynamic analysis is conducted for 280 seconds until shaking stops, and (b) consolidation is conducted over a period representing 150 years until EPWP dissipates completely. The initial stress field is calculated in advance via self-weight static analysis, and the values of initial stress for each element are shown in Figure 13. The value of the initial OCR is based on that of the initial stress and the clay's consolidation yield pressure. Figure 7 shows the input wave used in the simulation as applied at the bottom of the analytical domain. Stiffness proportional damping with a ratio of 5% was applied for the damping model, and the Newmark-β method was used for time integration.

Figures 7 through 9 show time histories of response acceleration at the ground surface, cumulative ground subsidence of the layer from the ground surface to a depth of 23 m and the excess pore water pressure ratio (EPWPR). It can be seen from these figures that response acceleration at the ground surface was amplified up to 500 Gal and that slight shaking lasted until 100 sec. Ground subsidence began to gradually increase soon after the shaking finished, showing close correspondence to the observation results, and continued for 150 years with a cumulative total of 250 mm. This subsidence was caused by the generation of EPWP in the shallow clayey layer due to shaking, and pressure dissipation took such a long time because of the ground's low permeability. Although EPWP generation was also observed in the silt layer, cumulative ground subsidence was less than that in the clayey layer because the compression and swelling index values and the degradation parameter of the over-consolidation state were smaller.

5 CONCLUSIONS

The findings of the study can be summarized as follows:

1. Ground subsidence observed before the 2007 Niigata Prefecture Chuetsu-Oki Earthquake was caused by ground water being pumped up.
2. The long-term subsidence observed after the quake can be explained by the generation of excess pore water pressure and its slow dissipation. This phenomenon was found to last for a long time due to low permeability and compression softening in the structured clay.
3. The seismic intensity of earthquakes has a significant influence on cumulative subsidence.
4. Based on the simulation results, excess pore water pressure conditions and ground subsidence can be expected to continue for more than 100 years after the tremblor.

6 REFERENCES

Asaoka, A., Nakano, M., Noda, T. and Kaneda K. 2000. Delayed compression/consolidation of natural clay due to degradation of soil structure. *Soils and Foundations* 40(3), 75-85.

Hashiguchi, K. and Ueno, M. 1977. Elastoplastic constitutive laws of granular material, Constitutive Equations of Soils. *Proc. 9th ICSMFE*, *Spec. Ses. 9 (eds. Murayama, S. and Schofield, A. N.)*, *Tokyo*, *JSSMFE*, 73-82.

Ye, B., Ye, G., Zhang, F. and Yashima, A. 2007. Experiment and numerical simulation of repeated liquefaction-consolidation of sand. *Soils and Foundations* 47(3), 547-558.

Zhang, F., Ye, B., Noda, T., Nakano, M. and Nakai, K. 2007. Explanation of cyclic mobility of soils: Approach by stress-induced anisotropy. *Soils and Foundations* 47(4), 635-648.

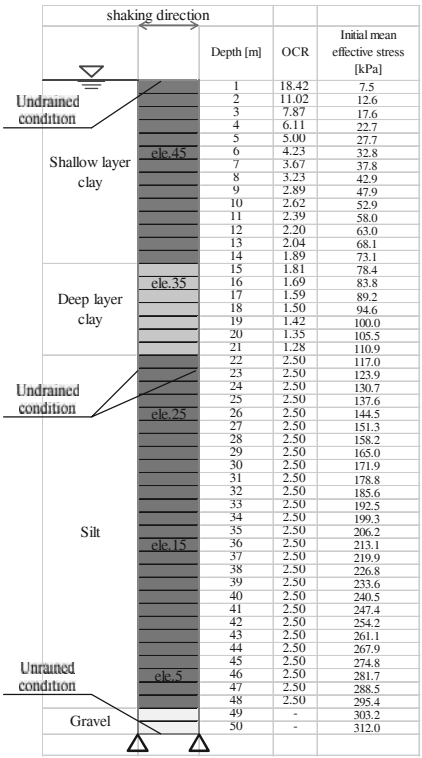

Figure 6. Finite element mesh and boundary conditions used in the simulation

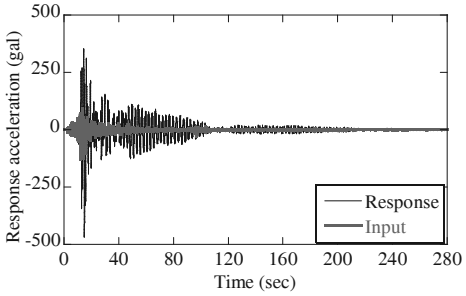

Figure 7. Time history of response acceleration on the surface

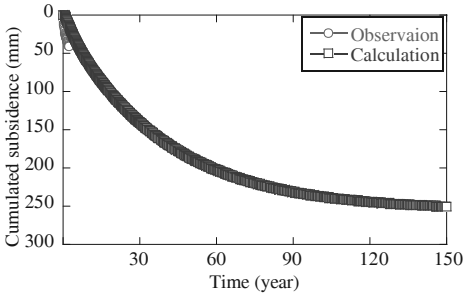

Figure 8 Time history of cumulative ground subsidence in the layer from the ground surface to a depth of 23 m

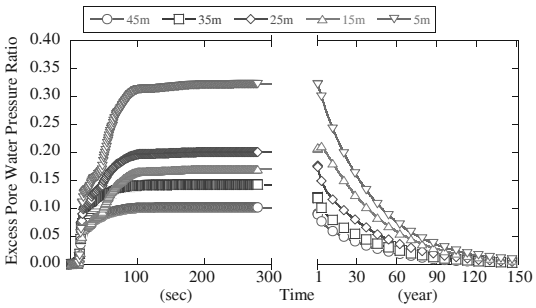

Figure 9. Time history of the excess pore water pressure ratio